CHEMISTRY OF MATERIALS

Article

pubs.acs.org/cm

Polyaniline/Vanadium Pentoxide Layer-by-Layer Electrodes for Energy Storage

Lin Shao,[†] Ju-Won Jeon,[‡] and Jodie L. Lutkenhaus*[,‡]

[†]Department of Chemical & Environmental Engineering, Yale University, New Haven, Connecticut 06511, United States

[‡]Department of Chemical Engineering, Texas A&M University, College Station, Texas 77843, United States

Supporting Information

ABSTRACT: Both polyaniline and vanadium pentoxide (V_2O_5) are promising electrode materials for electrochemical energy storage, but each has limitations. As a composite, the two components can interact synergistically to form an electrode better than either material alone. Using layer-by-layer (LbL) assembly as a processing technique, we successfully assembled hybrid electrodes containing polyaniline and V_2O_5. Assembly conditions were chosen to yield films that grew reliably and had a large cycle thickness. Assembly pH and concentration are critical parameters for this particular LbL system. For lower molar mass polyaniline, exponential film growth was observed; for higher molar mass polyaniline, linear growth was obtained. The electrochromic behavior of the film was characterized using UV−vis spectroscopy, and it was found that polyaniline dominated the electrochromic response. However, the electrochemical response possessed contributions from both polyaniline and V_2O_5. Films made from lower molar mass polyaniline had a charge storage capacity of 264 mAh/cm^3. The films' ability to store charge was also dependent on film thickness, as was the fraction of electrochemically accessible material. This work highlights how LbL assembly can be applied to produce intimately mixed electrodes containing both organic and inorganic materials.

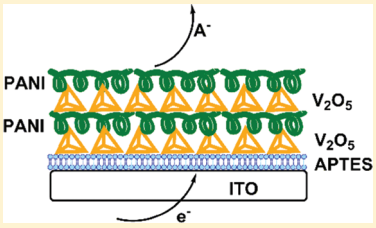

KEYWORDS: *layer-by-layer assembly, energy storage, polyaniline, vanadium pentoxide*

INTRODUCTION

Because of growing demand for low cost, high-performance portable power and energy storage technologies, innovative battery cathode materials and structures have attracted great interest.[1−5] These materials include transition-metal oxides,[6−11] metal dichalcogenides,[12−15] $LiFePO_4$,[16−18] $LiMn_2O_4$,[19−21] V_2O_5,[22−26] electronically conductive polymers,[27−29] and so on. The challenge is to balance conductivity, kinetics, diffusion, capacity, energy density, and power density within a given electrode. Of these various materials, electronically conductive polymers and V_2O_5 have attracted great interest because they excel in terms of some of the aforementioned challenges.

Electronically conductive polymers (e.g., polyacetylene, polythiophene, polypyrrole, polyaniline) have been investigated as organic cathodes for batteries for many years.[27−29] In 1987, coin-type polyaniline (PANI)-lithium secondary batteries were commercially available, but discontinued 5 years later.[30] Charge is stored through the doping (or dedoping) of anions into (or out of) the polyaniline electrode. In an inert, water-free environment the dominant reaction is the doping of leucoemeraldine base (LB) to emeraldine salt (ES) polyaniline and vice versa (Scheme 1a); protons are not expected to be major participants in nonaqueous environment. ES polyaniline is electronically conductive (σ = 2−5 S/cm),[31,32] and LB polyaniline is insulating. Accordingly, the theoretical capacity of the LB/ES reaction shown in Scheme 1a is 147 mAh/g, based on polyaniline based on the molar mass of the repeat unit.[33] Reported polyaniline-lithium cell potentials, capacities, and specific energies are in the range of 3 to 4 V, 100−147 mAh/g, and ∼300 mWh/g, respectively.[34−37] Specific powers are not often reported for polyaniline-lithium cells, but we have calculated a power density of ∼100 mW/g from one account.[38] Mass transfer of the anion A- is considered a rate-limiting factor.[28] Nevertheless, polyaniline is considered a promising electrode material because of its simple synthesis, high Coulombic efficiency (90−100%), good cyclability (>500 cycles), chemical stability, tunable properties, and low cost.[28,39]

Scheme 1. Redox Reactions for (a) PANI and (b) V_2O_5 in Non-Aqueous Solution

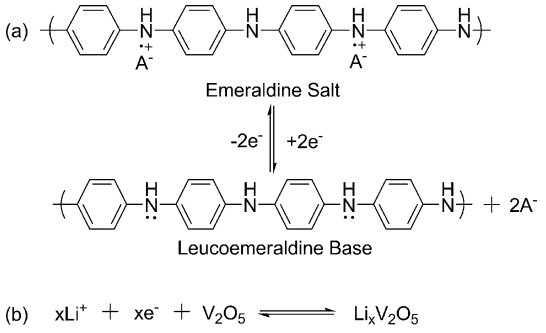

V_2O_5 has been investigated extensively as a promising cathode because of its high capacity and specific energy.[22−26,40,41] V_2O_5

Received: September 15, 2011
Revised: November 22, 2011
Published: November 24, 2011

stores energy through the intercalation of Li^+-ions during charge and discharge (Scheme 1b). Reported V_2O_5-lithium cell potentials, capacities, specific energies, and specific powers are in the range of 2 to 4 V, 500−650 mAh/g, 20−1600 mWh/g, and 50−1500 mW/g, respectively.[26,42,43] However, drawbacks include low conductivity,[41,44,45] low Li^+-diffusion coefficient,[46] volumetric expansion,[46,47] and performance fade.[44,48,49]

Polyaniline is often blended with electrochemically active inorganic battery materials, such as V_2O_5, with the motivation of synergistically enhancing aforementioned figures of merit. Electronically conductive polymers improve both conductivity and Li^+-ion diffusion in PANI/V_2O_5 composite electrodes. For example, the groups of Nazar[50,51] and Buttry[52] polymerized polyaniline in the presence of V_2O_5 to create inorganic/organic hybrid electrodes. The Li^+-diffusion coefficient for the PANI/V_2O_5 composite was 10 times that of V_2O_5 alone, and the capacity was also greater than V_2O_5 xerogel.[50] For this composite electrode, both reactions depicted in Scheme 1 occur simultaneously.

Layer-by-layer (LbL) assembly is a promising processing technique to prepare PANI/V_2O_5 composite electrodes. LbL assembly is the alternate exposure of a substrate to dilute solutions or dispersions of oppositely charged (or hydrogen bonding) molecules.[53,54] In the present work, PANI constitutes the positively charged species, and V_2O_5, which becomes a negatively charged polyvanadate in water, constitutes the polyanion. The LbL technique has been directed toward many energy applications such as batteries,[55−57] fuel cells,[58,59] and capacitors.[60−62] Here, PANI and V_2O_5 are alternately deposited as thin, molecularly intimate layers; therefore, LbL assembly potentially provides a synergistic processing technique to blend both materials. PANI/V_2O_5 LbL electrodes have been previously explored by the groups of Oliveira[63,64] and Knoll.[65] The areal capacity of the PANI/V_2O_5 LbL film was greater than the sum of the areal capacities from either material alone.[64,65] The film had an electrochemical response dominated by V_2O_5 and an electrochromic response dominated by PANI.[63] It was also reported that lithium ions were the mobile species within PANI/V_2O_5 LbL films, rather than bulky slow-moving anions.[63] Although promising as energy storage electrodes, PANI/V_2O_5 LbL films have not yet been fully explored; figures-of-merit such as capacity and cycle life and their relationship to film thickness and assembly parameters are not known. Furthermore, our own difficulty with reliably forming these films led us to investigate more optimal assembly conditions. Accordingly, this prior work motivated us to explore PANI/V_2O_5 LbL films as cathodes for lithium secondary batteries.

Here, we investigate PANI/V_2O_5 LbL films of various thickness, PANI molar mass, and assembly conditions and their influence on electrochemical energy storage. Whereas prior investigations have focused on a singular type of PANI/V_2O_5 LbL film, the present investigation explores multiple assembly parameters (pH, concentration, molar mass). We use UV−vis and Fourier Transform Infrared (FTIR) spectroscopy, zeta potential, dynamic light scattering (DLS), profilometry, cyclic voltammetry, and charge−discharge testing to quantify film growth, materials properties, and electrochemical activity. Results indicate that the type of film growth (linear vs exponential) is dependent on PANI molar mass. Successful film growth is dependent on assembly pH and the substrate's surface treatment. PANI/V_2O_5 LbL electrodes containing the lower molar mass PANI had a capacity of 264 mAh/cm^3 based on a current of 1 μA/cm^2. These LbL electrodes maintained up to 80% of its capacity over 500 cycles at a current of 20 μA/cm^2. The work presented here highlights that PANI/V_2O_5 LbL films are promising energy storage electrodes.

EXPERIMENTAL SECTION

Materials. Ammonium peroxydisulfate, aniline, commercially available emeraldine base PANI, ammonium hydroxide, (3-aminopropyl)-triethoxysilane (APTES), *N*-methyl-pyrrolidinone (NMP), propylene carbonate, lithium perchlorate, and dimethylacetamide (DMAc) were purchased from Sigma Aldrich. Vanadium triisopropoxide oxide was purchased from Gelest, Inc. Linear polyethylenimine (PEI, $M_w \sim$ 25,000) was purchased from Polysciences. Lithium ribbon was purchased from Alfa Aesar. All materials were used as received.

Substrates for LbL deposition include indium−tin oxide (ITO)-coated glass (Delta Technologies, resistance < 20 Ω) and quartz slides (Ted Pella, Inc.).

Polyaniline Synthesis and Dispersion Preparation. PANI synthesized in-house was compared to commercially available PANI. The synthesis is based on a previously reported method.[66] Twenty-five mmol ammonium peroxydisulfate was dissolved in 50 mL of 18.2 MΩ deionized water. Twenty mmol aniline was dissolved in 50 mL of 1 M HCl aqueous solution. Both solutions were stirred for 1 h at room temperature. Then, the ammonium peroxydisulfate solution was added slowly to the aniline solution. The mixture was stirred for 1 h at 5 °C. The precipitate, green ES polyaniline, was collected by filtration and washed repeatedly using 1 M HCl until the filtrate became colorless. The washed precipitate was dried under vacuum for 48 h.

ES polyaniline was converted to blue EB polyaniline by mixing with 0.1 M ammonium hydroxide.[67] Sonication was applied to assist this mixing process (three times, 10 h and fresh ammonium hydroxide solution for each time). Then, the precipitate was collected by filtration, washed using deionized water or water−methanol mixture, and dried under vacuum at room temperature for 24 h.

PANI dispersion was created following the method of Cheung et al.[68] First, 0.8 g of EB PANI was dissolved in 40 g of DMAc, followed by 12-h stirring and 10-h sonication. PANI solution was filtered using glass microfiber filters of 0.7 μm particle retention. The filtrate was then slowly added to pH 3−3.5 water until a volume ratio of 1:9 DMAc:H_2O was achieved to form a PANI dispersion. The pH of the dispersion was immediately adjusted to 2.5 using 1 M HCl. After another filtration step, the PANI dispersion was ready for use. However, the dispersion should be used within 2 days of preparation; after which, irreversible aggregation of PANI occurs.[68] The concentration of PANI within the dispersion was ~0.011 M based on repeat unit molar mass.

Vanadium Pentoxide Synthesis and Solution Preparation. V_2O_5 was prepared by an adaptation of a sol−gel method.[41,63] 1 mL of vanadium triisoproxide was added to 500 mL of deionized water. The solution was condensed using rotary evaporation at 60 °C until 250 mL of solution was left. The remaining orange solution had a pH of ~2.5 and a concentration of 0.0085 M V_2O_5. According to the phase diagram reported by Pelletier et al.,[69] the vanadium species present under these conditions is $V_{10}O_{26}(OH)_{24}^-$. In some cases, the solution was condensed until a red colloidal sol−gel was formed with a pH of 2. For simplicity we will call both types of solution, "V_2O_5 solution".

Preparation of PANI/V_2O_5 LbL Films. LbL films were constructed on ITO-coated glass and quartz substrates. Quartz slides were cleaned via sonication in piranha solution for 30 min and rinsed with copious deionized water. ***Caution!*** *Piranha solution is extremely corrosive and proper precautions must be taken.* The ITO-coated glass substrates were cleaned via sonication in dichloromethane, acetone, methanol, and deionized water for 15 min each. After cleaning, substrates were dried in a convection oven at 50 °C, followed by 5-min oxygen plasma treatment (Harrick PDC-32G).[70] Then, substrates were functionalized with APTES. Briefly, substrates were immersed in 2 vol % APTES in anhydrous toluene for 30 min at 75 °C. Then, the substrates were sequentially rinsed using toluene, ethanol, and deionized water, and dried at 110 °C for 15 min.[71] PANI/V_2O_5 LbL

dx.doi.org/10.1021/cm202774n | *Chem. Mater.* 2012, 24, 181−189

films were constructed using an automated slide stainer (HMS series, Carl Zeiss). APTES-functionalized substrates were immersed in V_2O_5 solution for 15 min followed by 2, 1, and 1 min successive rinsing steps in pH 2.5 water. The same procedure was then followed by exposure to PANI dispersion and rinsing as before. Films are designated as APTES(V_2O_5/PANI)$_n$ where subscript n denotes the number of layer pairs or cycles. LbL films were dried in ambient air following assembly. In some cases, ITO-coated glass substrates were treated with PEI or NMP instead of APTES functionalization. PEI treatment was performed by immersing substrates in pH 4, 20 mM PEI solution for 1 h. For NMP treatment, substrates were dipped in NMP for 2 s.

Materials Characterization. Molecular weight analysis of PANI was performed via gel permeation chromatography (GPC) using a Waters Alliance 2695 HPLC unit with NMP as the mobile phase at 50 °C with a flow rate of 1 mL/min. The results are relative to a poly(styrene) calibration curve (Intertek Analytical Sciences Americas Laboratory). Zeta potential and dynamic light scattering (DLS) (Nano ZS90, Malvern Instruments) were performed on PANI dispersion (water/DMAc mixture at pH 2.5) and V_2O_5 solution. UV−vis absorption spectra of EB polyaniline solution in DMAc, ES polyaniline dispersion in water/DMAc mixture at pH 2.5, and APTES(V_2O_5/PANI) LbL films on quartz and ITO-coated glass slides were recorded using a Hitachi U-4100 spectrophotometer. The thickness of APTES(V_2O_5/PANI) LbL films on ITO-coated glass was measured using a profilometer (*P*-6 KLA-Tencor). The thickness of each sample was the average of at least 10 selected points. APTES(V_2O_5/PANI) LbL films were characterized using an FTIR spectrometer (Bruker Optics, ALPHA-P 10098-4). Absorption spectra were taken in attenuated total reflectance (ATR)-mode by averaging 1,024 scans at 2 cm^{-1} resolution. The composition of APTES(V_2O_5/PANI) LbL films was investigated using X-ray photoelectron spectroscopy (XPS), (Kratos Axis Ultra DLD photoelectron spectrometer with a resolution 0.1 eV). The instrument used a monochromatic Al X-ray source at a pass energy of 40 eV and a charge neutralizer. The analyzed area was 700 × 300 μm. The take-off angle was 90 degrees and the acceleration voltage was 12 kV. The N1s and V2p peaks were at 399.95 and 576.45 eV respectively.

Electrochemical Characterization. Dried APTES(V_2O_5/PANI)$_n$ LbL films were electrochemically investigated using a three-electrode cell in an oxygen-free, water-free, argon-filled glovebox. LbL film on ITO-coated glass was the working electrode, and two lithium ribbons acted as counter and reference electrodes. The electrolyte was 0.5 M $LiClO_4$ in propylene carbonate. All electrochemical tests were performed using a Solartron SI 1287 at room temperature.

RESULTS

Characterization of PANI and V_2O_5. PANI synthesized in-house (H-PANI) was compared to commercially available PANI (C-PANI). Table 1 shows the weight-average molar mass (M_w), polydispersity index (PDI), hydrodynamic diameter (D_h), and zeta potential of H-PANI and C-PANI. The weight-average molar mass and PDI of H-PANI is greater than that of C-PANI. Correspondingly, the particle size of H-PANI is larger than that of C-PANI in dispersion. However, the zeta potentials of both H-PANI and C-PANI dispersion are similar. The zeta potential and D_h of V_2O_5 (pH 2.5, 0.0085 M) were −25 mV and 159 nm, respectively.

Table 1. Comparison of Commercial PANI (C-PANI) and Home-Made PANI (H-PANI)

	M_w (g/mol)	PDI	Zeta potential (mV)	D_h (nm)
C-PANI	8,440	3.3	+45	100
H-PANI	20,880	5.3	+49	307

UV−vis spectra of V_2O_5 solution, ES (green) and EB (blue) H-PANI are shown in Figure 1. V_2O_5 solution exhibits a sharp shoulder around 500 nm.[72] EB H-PANI shows two peaks at 330 and 630 nm, which are attributed to the excitation of amine and imine groups, respectively.[73] For ES H-PANI in pH 2.5 DMAc/water mixture, the peak at 630 nm shifts to 900 nm. A small shoulder around 630 nm is present, likely because PANI is partially protonated.[73] Spectra for C-PANI were identical to those of H-PANI.

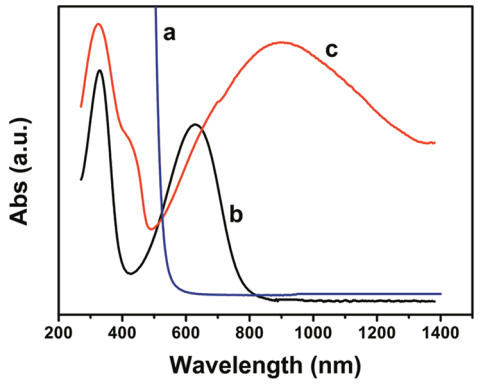

Figure 1. UV−vis spectra of (a) V_2O_5 solution at pH 2.5, (b) EB H-PANI in DMAc, and (c) H-PANI at pH 2.5 in water/DMAc mixture.

LbL Assembly of PANI and V_2O_5. In prior work,[63−65,74] LbL assemblies of PANI and V_2O_5 were reportedly assembled at pH 2, where V_2O_5 concentration was 0.04 M. Initially we carried out LbL assembly at identical conditions, but growth was not uniform or successful, as indicated by UV−vis spectroscopy (Supporting Information, Figure S1). On the basis of the research of Pelletier et al.[69] and Cheung et al.,[68] we hypothesize that the failure of PANI/V_2O_5 LbL assembly at pH 2 might be attributed to insufficient electrostatic interactions and to aggregation of H-PANI. V_2O_5 in water has a complex phase diagram, where vanadium pentoxide can form neutral ribbon-like colloids, or negatively or positively charged polyvanadate ions under various concentrations and pH values.[69] Under the preceding conditions (pH 2, 0.04 M), the dominant species is expected to be V_2O_5 colloid;[69] zeta potential indicated that the V_2O_5 colloid is weakly charged (less than −10 mV), but the data were somewhat unreliable. While prior work successfully deposited LbL films at these conditions, it is possible that the actual pH or concentration was slightly closer to a region where negatively charged polyvanadates existed.

With the motivation of reducing PANI aggregation and encouraging the formation of negatively charged polyvanadates, the pH of all assembly baths was set at 2.5, and V_2O_5 concentration was 0.0085 M. At these conditions, the dominant species in V_2O_5 solution is $V_{10}O_{26}(OH)_{24}^{-}$.[69] Successful LbL assembly was confirmed via UV−vis spectroscopy and profilometry, (Figures 2 and 3, respectively). Both absorbance and thickness increase monotonically with each cycle of LbL assembly. We hypothesize that the successful assembly is primarily driven by electrostatic interactions between positively charged PANI particles and negatively charged $V_{10}O_{26}(OH)_{24}^{-}$. To test this hypothesis, we carried out LbL assembly using only PANI (without V_2O_5 solution); as expected, there was no observable growth, (Supporting Information, Figure S2).

The UV−vis spectra of APTES(V_2O_5/PANI)$_n$ LbL films on quartz are shown in Figure 2. Compared with Figure 1, the ES-PANI peak at 900 nm shifted to a lower wavelength (828 nm) and broadened for the LbL film, suggesting that both ES and EB PANI exist in the LbL film. The partial conversion of ES to

dx.doi.org/10.1021/cm202774n | *Chem. Mater.* 2012, 24, 181−189

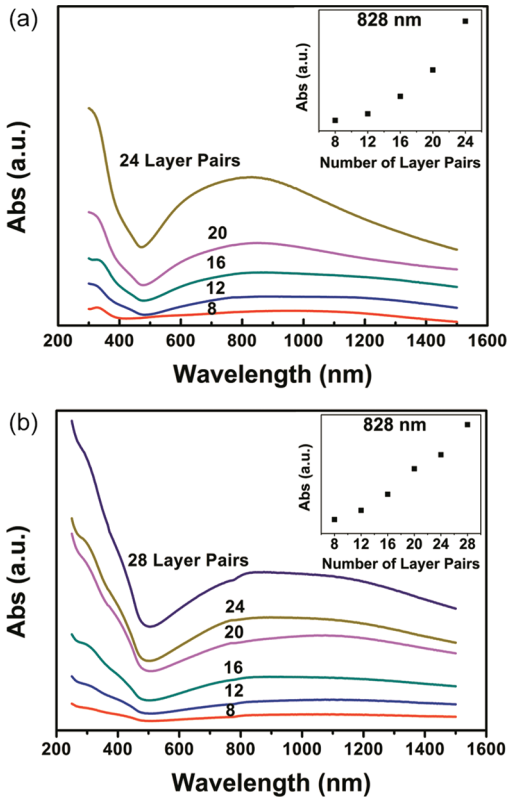

Figure 2. UV−vis spectra of (a) APTES(V_2O_5/C-PANI)$_n$ and (b) APTES(V_2O_5/H-PANI)$_n$ LbL films on quartz. The insets are the UV-absorption values at 828 nm vs number of layer pairs.

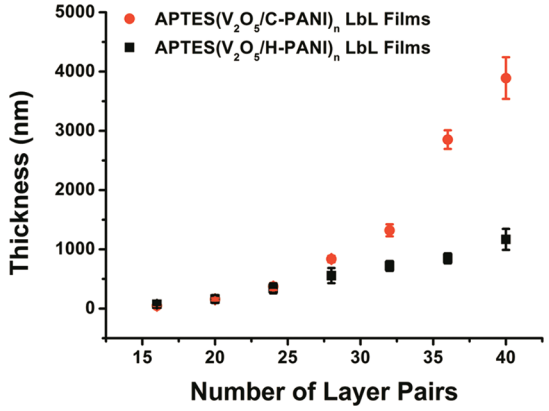

Figure 3. Growth profile of APTES(V_2O_5/PANI)$_n$ LbL films on ITO-coated glass slides for H-PANI (red circles) and C-PANI (black squares).

EB PANI has been observed elsewhere for LbL films, and is attributed to strong interactions between PANI and V_2O_5.[74] The insets of Figures 2a and b describe the absorbance intensity at 828 nm as a function of number of layer pairs. APTES(V_2O_5/C-PANI)$_n$ and APTES(V_2O_5/H-PANI)$_n$ LbL films grew exponentially and linearly, respectively. Peaks associated with V_2O_5 were not observed. The films grew visibly darker with increasing number of layer pairs, Supporting Information, Figures S3 and S4.

Figure 3 shows growth profiles of APTES(V_2O_5/PANI)$_n$ LbL films fabricated using C-PANI and H-PANI dispersion measured using profilometry. Similar to UV−vis spectra, the thickness of APTES(V_2O_5/H-PANI)$_n$ LbL films increased linearly with the number of layer pairs (39.6 nm/layer pair), and the thickness of APTES(V_2O_5/C-PANI)n LbL films increased exponentially. This striking difference between linear and exponential growth is possibly attributed to differences between molar mass and particle size between C-PANI and H-PANI.[75−77]

ATR-FTIR spectra confirm the presence of both PANI and V_2O_5 within the PANI/V_2O_5 LbL film, Figure 4. Peaks

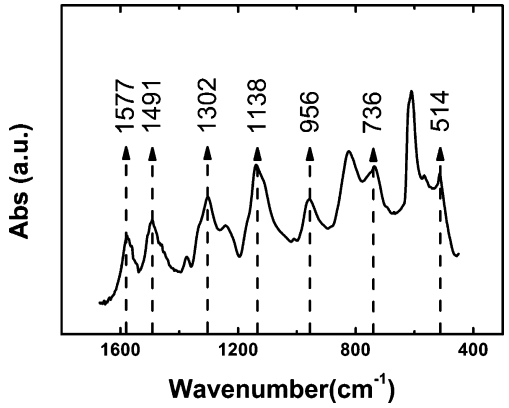

Figure 4. ATR-FTIR spectra of APTES(V_2O_5/H-PANI)$_{32}$ LbL films.

observed at 514, 736, and 956 cm^{-1} are attributed to symmetric V−O−V stretching, asymmetric V−O stretching, and V═O vibration.[52,74] Peaks observed at 1138 cm^{-1} and 1302 cm^{-1} are attributed to C−H bending and C−N stretching, respectively.[52,74] C═C stretching in quinoid and benzenoid segments is assigned to peaks at 1491 cm^{-1} and 1577 cm^{-1}, respectively.[52,74]

It should be noted that other surface treatments were attempted in place of APTES. ITO can be a challenging surface for LbL assembly, and the addition of a surface layer to promote LbL growth is a common practice. We explored linear PEI, NMP, and APTES as surface layers, and concluded that APTES provided for uniform LbL growth. PEI and NMP treatments encourage LbL growth, but not in a uniform or regular manner (Supporting Information, Figures S5 to S7).

Electrochemical Characterization of APTES(V_2O_5/PANI)$_n$ LbL Films. With a reproducible protocol in place for building PANI/V_2O_5 LbL electrodes, we next sought to explore their electrochemical energy storage capabilities. Electrochemical characterization of APTES(V_2O_5/PANI)$_n$ LbL films of varying layer pair number was performed under an inert atmosphere in a nonaqueous electrolyte. Cyclic voltammetry, galvanostatic charge−discharge testing, and cycling were performed. Because the LbL electrode contains both PANI and V_2O_5, it is expected that both electrochemical reactions depicted in Scheme 1 will contribute to the electrode's electrochemical response.

Cyclic Voltammetry. The electrochemical behavior of APTES(V_2O_5/C-PANI)$_n$ and APTES(V_2O_5/H-PANI)$_n$ LbL films was investigated using cyclic voltammetry, Figure 5. Both types of LbL films have voltammograms of similar shape. Anodic scans have a single peak followed by a capacitive plateau at higher potentials. Cathodic scans also have a single peak that is symmetric with the anodic scan, indicating reversibility. The peaks around 3 V are attributed to the reduction/oxidation of PANI (LB/ES) and V_2O_5 (V^{4+}/V^{5+}), and the plateaus in the cathodic scan from 3.1 to 3.5 V are assigned to PANI.[50,64,78]

dx.doi.org/10.1021/cm202774n | *Chem. Mater.* 2012, 24, 181−189

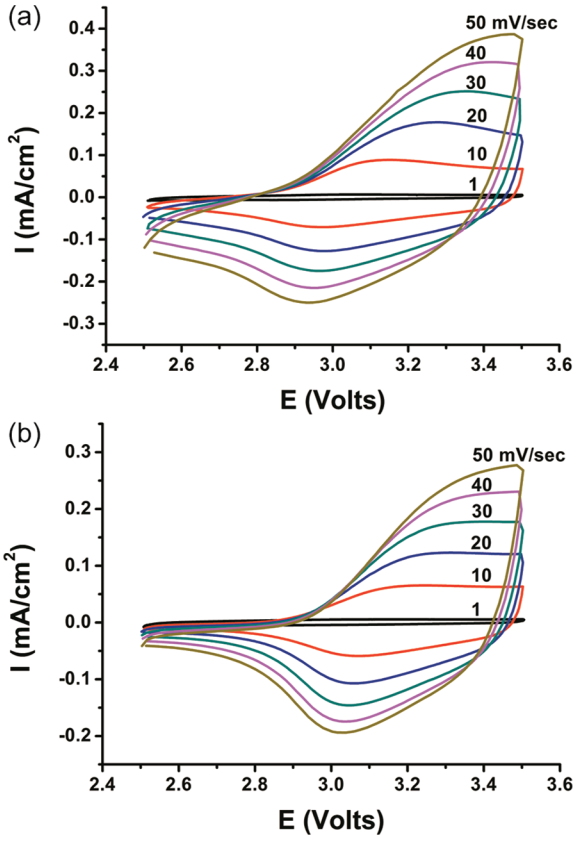

Figure 5. Cyclic voltammograms of (a) APTES$(V_2O_5$/C-PANI$)_{16}$ and (b) APTES$(V_2O_5$/H-PANI$)_{16}$ LbL films with different scan rates. Potential is vs Li/Li^+.

To better understand this redox reaction, we conducted UV−vis spectroscopy to monitor the electrochromic activity of the LbL electrodes, Figure 6. At 3.5 V PANI is oxidized into the

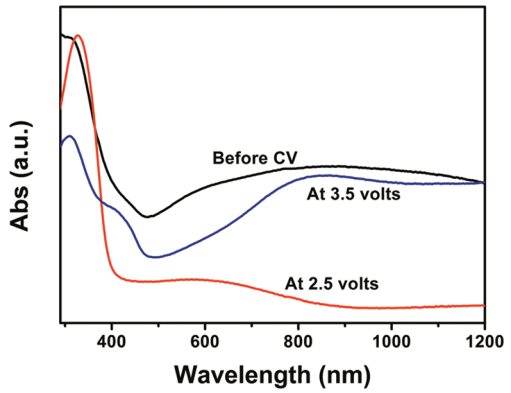

Figure 6. (a) UV−vis spectra of APTES$(V_2O_5$/C-PANI$)_{16}$ LbL films before CV (black curve), at 2.5 V (red curve), and at 3.5 V (blue curve).

ES state, confirmed by the broad peak at 830 nm. At 2.5 V, PANI is reduced to the LB state and the peak disappears. Again, no obvious signal from vanadium species was observed. Over the visible region from 390 to 780 nm, the extinction coefficient of V_2O_5 decreases from 0.25 to around zero with increasing wavelength; for PANI, the extinction coefficient decreases from 0.5 to 0.06 with increasing wavelength from 390 to 660 nm, followed by an increase up to 0.4 at 780 nm.[79,80] Therefore, the electrochromic activity of the film appears to be dominated by PANI.

The prior experiment explored LbL films of constant layer pair number under varying scan rate, but it is interesting to explore the converse, where layer pair number varies and scan rate is constant. Such an experiment illustrates the influence of film thickness on the electrochemistry. Figures 7a and b show

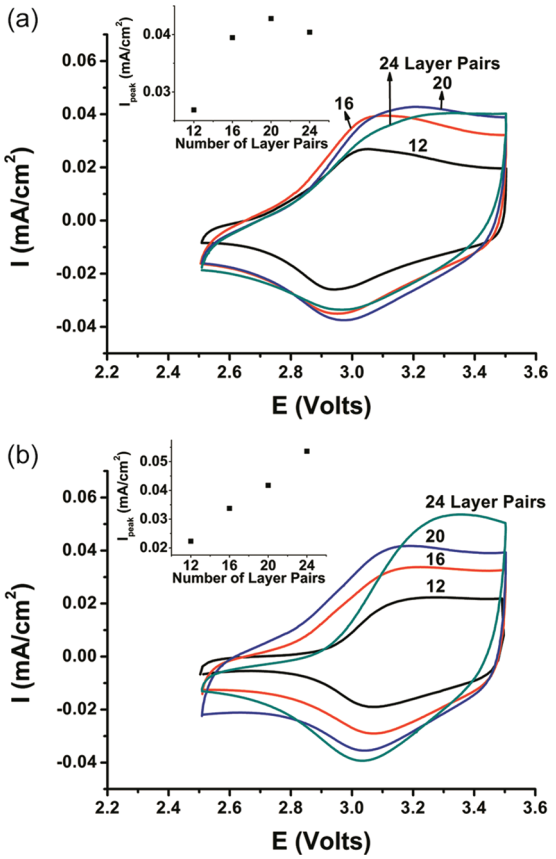

Figure 7. Cyclic voltammograms of (a) APTES$(V_2O_5$/C-PANI$)_n$ and (b) APTES$(V_2O_5$/H-PANI$)_n$ LbL films with varying number of layer pairs at a scan rate of 5 mV/s. Potential is vs Li/Li^+.

cyclic voltammograms for APTES$(V_2O_5$/PANI$)_n$ LbL films, where n is varied from 12 to 24 layer pairs and the scan rate is constant at 5 mV/s. For APTES$(V_2O_5$/C-PANI$)_n$ LbL films (Figure 7a), the peaks shift to higher voltages in the anodic scan and shift to lower voltages in the cathodic scan. The peak current increased with increasing thickness up to 16 layer pairs and saturated at approximately 20 layer pairs, (inset of Figure 7a). We hypothesize that this is caused by a shift from a surface-confined process to a diffusion-limited process. For APTES-$(V_2O_5$/H-PANI$)_n$ LbL films (Figure 7b), the voltage shifts in the peaks in the cathodic and anodic scans show a similar trend. However, the peak current did not show saturation with increasing thickness; instead, peak current increases linearly with layer pair number for H-PANI-containg LbL films, (inset of Figure 7b). We hypothesize this resulted from the easy penetration of electrolyte into APTES$(V_2O_5$/H-PANI$)_n$ LbL films compared to APTES$(V_2O_5$/C-PANI$)_n$ LbL films with the same layer pairs.

Charge/Discharge Testing. Typical charge−discharge profiles for APTES$(V_2O_5$/C-PANI$)_{16}$ and APTES$(V_2O_5$/H-PANI$)_{16}$ LbL electrodes are illustrated in Figures 8a and 8c.

dx.doi.org/10.1021/cm202774n | *Chem. Mater.* 2012, 24, 181−189

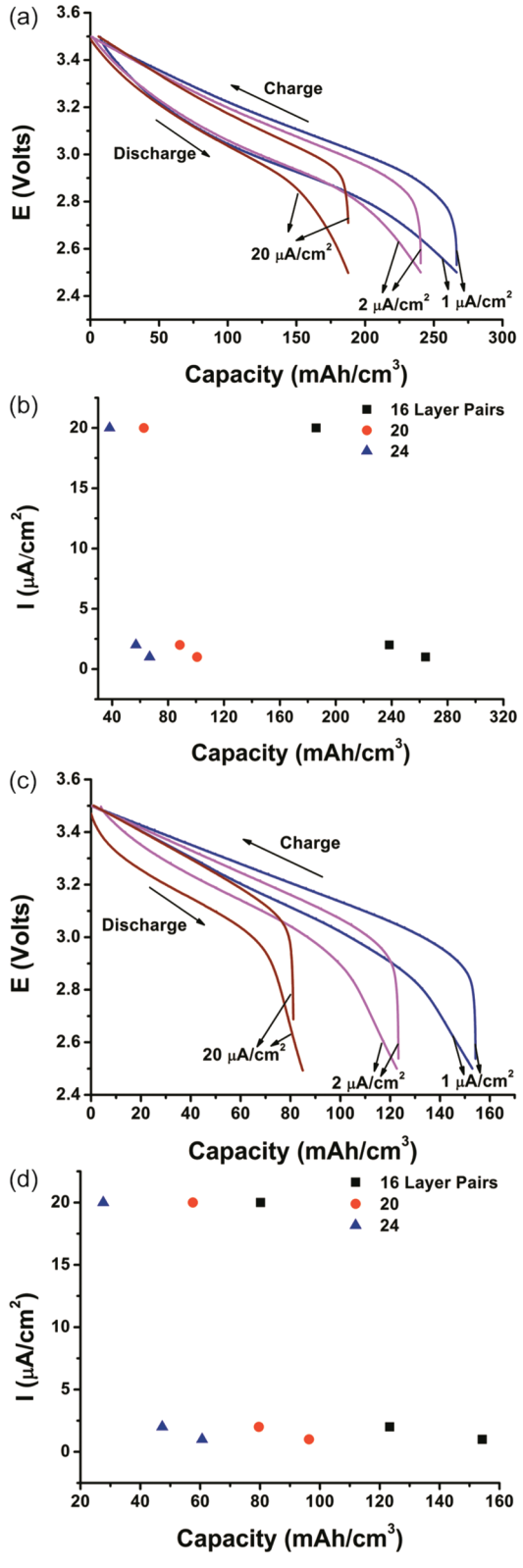

Figure 8. Galvanostatic charging and discharging of (a) APTES$(V_2O_5$/C-PANI$)_{16}$ and (c) APTES$(V_2O_5$/H-PANI$)_{16}$ LbL films. Capacities under various charging currents (1, 2, 20 μA/cm^2) for (b) APTES$(V_2O_5$/C-PANI$)_n$ and (d) APTES$(V_2O_5$/H-PANI$)_n$ LbL films, where n = 16, 20, or 24 layer pairs.

As expected, capacity increases with decreasing current. The shape of the charge–discharge profile is sloping, a typical feature of polymer electrodes.[28] Figures 8b and d show the dependence of capacity on number of layer pairs and dicharge current. The largest capacity observed for APTES$(V_2O_5$/C-PANI$)_n$ LbL films was 264 mAh/cm^3 for a charging current of 1 μA/cm^2 and n = 16. Also, the largest capacity observed for APTES$(V_2O_5$/H-PANI$)_n$ LbL films was 158 mAh/cm^3 for a charging current of 1 μA/cm^2 and n = 16. Interestingly, thicker films (20, 24 layer pairs) have diminished capacity relative to the thinner 16 layer pair films. We speculate that thicker films are more susceptible to diffusion limitations, thus limiting overall capacity.

The cycle life of both APTES$(V_2O_5$/C-PANI$)_n$ and APTES-$(V_2O_5$/H-PANI$)_n$ LbL electrodes of varying layer pair number was examined over multiple charge–discharge cycles at a charging current of 20 μA/cm^2, Figures 9 and 10. For

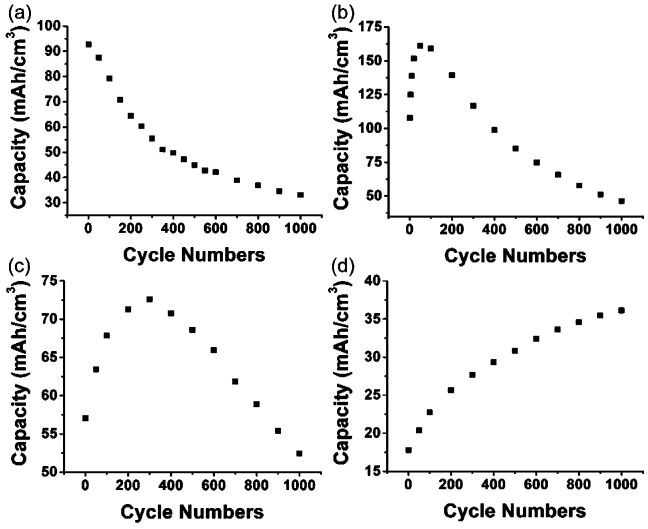

Figure 9. Capacity vs number of cycles for APTES$(V_2O_5$/C-PANI$)_n$ LbL films where n = (a) 12, (b) 16, (c) 20, or (d) 24 layer pairs at a constant current of 20 μA/cm^2.

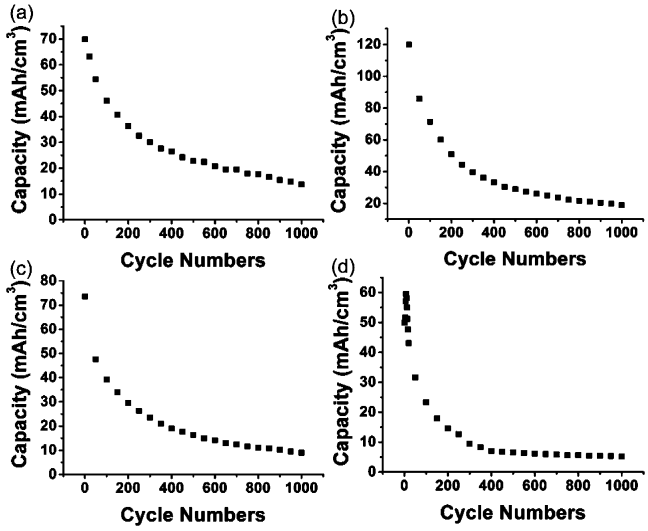

Figure 10. Capacity vs number of cycles for APTES$(V_2O_5$/H-PANI$)_n$ LbL films where n = (a) 12, (b) 16, (c) 20, or (d) 24 layer pairs at a constant current of 20 μA/cm^2.

APTES$(V_2O_5$/C-PANI$)_n$ LbL films, when n = 12, the capacity decreases 65% over 1000 cycles, Figure 9a. When n = 16 or 20, the capacity first increases and then decreases, Figures 9b and c. This behavior has been observed elsewhere and is associated

dx.doi.org/10.1021/cm202774n | *Chem. Mater.* 2012, 24, 181–189

with the penetration of electrolyte into the electrode during cycling.[34] The sample with n = 16 exhibited optimum performance (Figure 9b); the capacity increased from 108 to 166 mAh/cm^3 during the first 50 cycles, and then decreased to 47 mAh/cm^3 after 1,000 cycles. When n = 24, capacity continually increases with cycling, Figure 9d.

These results suggest that electrolyte penetration (which facilitates the redox reaction and enhances capacity) competes with electrode degradation. Thinner films are more likely to be saturated with electrolyte, so degradation dominates during cycling, whereas thicker films show the opposite case. Electrode degradation likely results from the irreversible formation of pernigraniline base (PB) polyaniline. To test this hypothesis, we performed UV−vis spectroscopy on electrodes before and after cycling, Supporting Information, Figure S8. At the 1000th cycle, the electrode showed evidence of PB formation, where the peak at 628 cm^{-1} had shifted to 580 cm^{-1}. Another mechanism for apparent capacity fade is volumetric expansion, Supporting Information, Figure S9.

For APTES(V_2O_5/H-PANI)$_n$ LbL films, n = 12, 16, 20 (Figure 10), the capacity steadily decreased with cycling. When n = 12, capacity decreased from 70 to 14 mAh/cm^3; when n = 16, capacity decreased from 120 to 18.7 mAh/cm^3; and when n = 20, capacity decreased from 73.5 to 9 mAh/cm^3. The thicker film, where n = 24, had a slight increase of capacity during the first 10 cycles from 50 to 60 mAh/cm^3, followed by a decrease to 5 mAh/cm^3.

DISCUSSION

By simply changing the molar mass of PANI used for LbL assembly, two very different kinds of films have been formed. Low molar mass C-PANI yielded exponential LbL growth, and higher molar mass H-PANI yielded linear LbL growth. Linear and exponential growth of LbL films have been reported by many groups.[75−77] According to those reports, exponential growth results from (i) an increase of surface roughness of a newly deposited layer[81−83] or (ii) the diffusion of adsorbing species into and out of the film.[77,84,85] The former phenomena has been associated with some colloid-containing LbL assemblies, where the globular nature of the colloid increases surface roughness, which, in turn, increases the amount of material adsorbed in the next step. If this were the case, then one might expect to observe exponential growth for the higher molar mass H-PANI, but we observe quite the opposite. Instead, lower molar mass PANI exhibits exponential growth. This indicates that the latter phenomenon is responsible for exponential growth in this system. The lower molar mass C-PANI has a smaller size, which facilitates the "in and out" diffusion of polyelectrolyte responsible for exponential growth. Accordingly, larger sized H-PANI is less diffusive, and exhibits linear growth.

For the linearly growing APTES(V_2O_5/H-PANI)$_n$ LbL film, the growth rate was 39.6 nm/layer pair. In contrast, Ferreira et al. observed a linear growth rate of 2.5 nm/layer pair.[64] We attribute the 10-fold difference to the pHs selected for assembly and the difference in V_2O_5 concentration. Ferreira et al. used assembly pH 2, and the present study used pH 2.5. As mentioned earlier, we were unable to assemble films at pH 2, which may be caused by V_2O_5's low charge at pH 2.

One might expect that C-PANI/V_2O_5 and H-PANI/V_2O_5 LbL films of comparable thickness would yield similar electrochemical capacities based on having similar volumes. However, this is not the case; although both LbL films with n = 16 have similar thickness (60 nm), their capacities are quite different, (Figures 8a and c). This may be attributed to differences in density, composition, and PANI particle size between the two types of films. X-ray photoelectron spectroscopy was applied to investigate the composition of LbL films containing C-PANI or H-PANI. APTES(V_2O_5/C-PANI)$_{20}$ LbL films were 62.5 mol % V_2O_5 (or 45 wt %), and APTES(V_2O_5/H-PANI)$_{20}$ LbL films were 73.4 mol % V_2O_5 (or 58 wt %). One might expect APTES(V_2O_5/H-PANI)$_{20}$ LbL films to have higher capacity because of the higher V_2O_5-content; however, this is not the case (Figures 8b and d). On the other hand, the larger polyaniline content in the C-PANI LbL films relative to H-PANI LbL films may enhance conductivity, leading to a higher capacity.

Another possible reason for films of identical thickness to have different capacities could arise from the amount of material that is electrochemically accessible or active. However, on the basis of the following discussion, we observe that both types of films have similar electrochemical accessibility for n = 16. Because the oxidation state of PANI is easily observed using UV−vis spectroscopy, we define a parameter describing the fraction of electrochemically accessible PANI as $(A_{3.5} - A_{2.5})/A_{3.5}$, where $A_{3.5}$ and $A_{2.5}$ are the absorbance (at 828 nm) of films at 3.5 and 2.5 V, respectively, during cyclic voltammetry (1 mV/s). For example, $(A_{3.5} - A_{2.5})/A_{3.5}$ may be calculated from Figure 6 where the film switches between ES and LB polyaniline at 3.5 and 2.5 V, respectively.

Figure 11 shows how the fraction of electrochemically accessible PANI varies with layer pair number (or thickness).

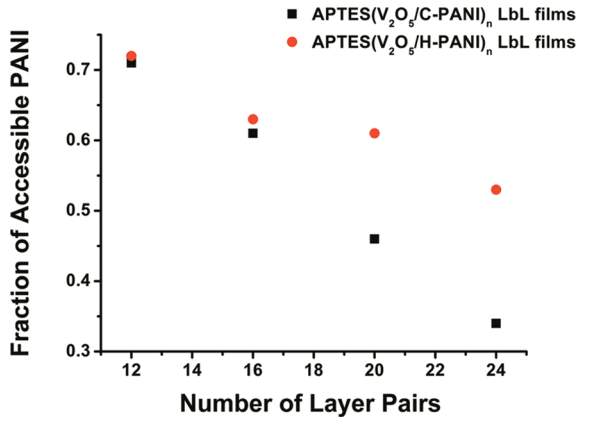

Figure 11. Fraction of electrochemically accessible PANI in APTES(V_2O_5/C-PANI)$_n$ (black squares) and APTES(V_2O_5/H-PANI)$_n$ LbL films (red circles).

Overall, the fraction of PANI available for electrochemical reaction decreases as thickness increases. This trend is supported by cyclic voltammetry, where thicker films are more susceptible to diffusion limitations. LbL films containing H-PANI have a higher fraction of accessible PANI relative to LbL films containing C-PANI. In the range studied (12 to 24 layer pairs) the thickness of the C-PANI and H-PANI-containing LbL films were similar, so thickness does not appear to play a role on accessibility (at least in initial cycles).

We also speculate that differences in accessibility are attributed to film morphology (density, pore structure). Here, the film morphology may be affected by the size of PANI colloid depositing on the surface. From DLS, C-PANI is much smaller than H-PANI, Table 1. C-PANI may adsorb in a layer more densely packed than H-PANI. If this were the case, then

dx.doi.org/10.1021/cm202774n | Chem. Mater. 2012, 24, 181−189

penetration of electrolyte into the electrode interior would be a challenge for LbL films containing C-PANI. Supporting this notion, repeated cycling of LbL films containing C-PANI shows evidence for hindered electrolyte penetration, (Figure 9). Future studies will examine density and composition quantitatively via quartz crystal microbalance.

The prior analysis can also aid in explaining the behavior of capacity with cycle number (Figure 9). For thin films where n = 12 layer pairs, the films have an initially high fraction of electrochemically accessible material; with cycling, PANI is irreversibly converted to PB PANI, and the accessible fraction steadily decreases, as does capacity. For much thicker films where n = 24 layer pairs, the films have a low fraction of accessible material; with repeated cycling, electrolyte penetrates into the film and allows for more and more PANI to be available. Correspondingly, capacity steadily increases with cycling. At intermediate thickness where n = 16 and 20, mixed behavior is observed.

As discussed previously, we understand that the irreversible oxidation of LB to PB PANI may lead to the fading during cycling. However, it is not the only factor to affect cycle life. Changes in volume may also play an important role on capacity fade. It is well-known that volume expansion is a common issue for various cathode materials in lithium-ion batteries.[1,4,86] For our APTES$(V_2O_5/PANI)_n$ LbL film electrodes, we also observed a change in volume (Supporting Information, Figure S9) after repeated cycling, which is possibly related to volume expansion associated with V_2O_5[46,47] and electrolyte penetration. For a 16 layer pair film containing C-PANI or H-PANI, thickness increased by 169% or 61%, respectively.

From Figure 8b and 9b, we noted that APTES$(V_2O_5/PANI)_{16}$ LbL film electrode appears the optimum performance. The capacity of this LbL electrode was 264 mAh/cm^3 based on current of 1 μA/cm^2. After 500 cycles this electrode retained 80% of the initial capacity at a current of 20 μA/cm^2. The observed capacity is far larger than the theoretical capacity of polyaniline (124 mAh/cm^3, including the perchlorate anion and assuming a polyaniline density of 1.3 g/cm^3). Therefore, V_2O_5 must also be participating in reaction as it has a much larger capacity. This synergistic effect suggests that both materials are simultaneously storing charge in the electrode.

CONCLUSIONS

Polyaniline and V_2O_5 were combined using layer-by-layer assembly to form a composite cathode for electrochemical energy storage. The PANI/V_2O_5 electrode was optimized with respect to assembly pH, assembly concentration, polyaniline molar mass, and surface treatment. Under optimum conditions, LbL films show exponential or linear growth for PANI of low or high molar mass, respectively. The LbL films have an electrochromic response dominated by polyaniline, and an electrochemical response from both PANI and V_2O_5. The capacity and charge−discharge behavior can be controlled by the number of layer pairs, where thicker films have diffusion-limitations. The best-performing electrode was made from lower molar mass PANI (C-PANI) and consisted of 16 layer pairs; the capacity was 264 mAh/cm^3 based on 1 μA/cm^2. After 500 cycles, the electrode maintained 80% of its original capacity at a discharge current of 20 μA/cm^2. Irreversible oxidation of LB to PB PANI and volume expansion contribute to the degradation of performance. Further research entails the investigation of the influence of PANI/V_2O_5 LbL morphology, such as nanostructured surfaces, on electrochemical performance. Our work opens up a new insight in the development of high-performance electrodes in flexible and thin film batteries.

ASSOCIATED CONTENT

Supporting Information

UV−vis spectra of LbL films assembled under alternative conditions. UV−vis spectra before and after cycling. Volumetric expansion after cycling. This material is available free of charge via the Internet at http://pubs.acs.org.

AUTHOR INFORMATION

Corresponding Author

*E-mail: jodie.lutkenhaus@che.tamu.edu.

ACKNOWLEDGMENTS

We thank the National Science Foundation (#0938842) and the Welch Foundation for financial support. We thank Dr. Nicole Zacharia for profilometer and FTIR spectrometer access, and Dr. Akbulut for DLS and zeta potential access. We also thank the TAMU Materials Characterization Facility.

REFERENCES

(1) Tarascon, J. M.; Armand, M. *Nature* **2001**, *414*, 359.
(2) Whittingham, M. S. *Chem. Rev.* **2004**, *104*, 4271.
(3) Winter, M.; Besenhard, J. O.; Spahr, M. E.; Novak, P. *Adv. Mater.* **1998**, *10*, 725.
(4) Whittingham, M. S. *MRS Bull.* **2008**, *33*, 411.
(5) Scrosati, B.; Garche, J. *J. Power Sources* **2010**, *195*, 2419.
(6) Kobayash., K.; Kosuge, K.; Kachi, S. *Mater. Res. Bull.* **1969**, *4*, 95.
(7) Liao, C. L.; Wu, M. T.; Yen, J. H.; Leu, I. C.; Fung, K. Z. *J. Alloys Compds.* **2006**, *414*, 302.
(8) Han, S. C.; Kim, H. S.; Song, M. S.; Lee, P. S.; Lee, J. Y.; Ahn, H. J. *J. Alloys Compds.* **2003**, *349*, 290.
(9) Yamaki, J.; Makidera, M.; Kawamura, T.; Egashira, M.; Okada, S. *J. Power Sources* **2006**, *153*, 245.
(10) Liu, P.; Lee, S. H.; Yan, Y. F.; Tracy, C. E.; Turner, J. A. *J. Power Sources* **2006**, *158*, 659.
(11) Yamada, K.; Sato, N.; Fujino, T.; Lee, C. G.; Uchida, I.; Selman, J. R. *J. Solid State Electrochem.* **1999**, *3*, 148.
(12) Desilvestro, J.; Haas, O. *J. Electrochem. Soc.* **1990**, *137*, C5.
(13) Han, S. C.; Kim, H. S.; Song, M. S.; Kim, J. H.; Ahn, H. J.; Lee, J. Y. *J. Alloys Compds.* **2003**, *351*, 273.
(14) Whittingham, M. S. *Prog. Solid State Chem.* **1978**, *12*, 41.
(15) Jacobson, A. J.; Chianelli, R. R.; Whittingham, M. S. *J. Electrochem. Soc.* **1979**, *126*, 2277.
(16) Padhi, A. K.; Nanjundaswamy, K. S.; Goodenough, J. B. *J. Electrochem. Soc.* **1997**, *144*, 1188.
(17) Huang, H.; Yin, S. C.; Nazar, L. F. *Electrochem. Solid-State Lett.* **2001**, *4*, A170.
(18) Chang, H. H.; Chang, C. C.; Wu, H. C.; Guo, Z. Z.; Yang, M. H.; Chiang, Y. P.; Sheu, H. S.; Wu, N. L. *J. Power Sources* **2006**, *158*, 550.
(19) Shen, P. Z.; Jia, D. Z.; Huang, Y. D.; Liu, L.; Guo, Z. P. *J. Power Sources* **2006**, *158*, 608.
(20) Tu, J.; Zhao, X. B.; Xie, J.; Cao, G. S.; Zhuang, D. G.; Zhu, T. J.; Tu, J. P. *J. Alloys Compds.* **2007**, *432*, 313.
(21) Shigemura, H.; Sakaebe, H.; Kageyama, H.; Kobayashi, H.; West, A. R.; Kanno, R.; Morimoto, S.; Nasu, S.; Tabuchi, M. *J. Electrochem. Soc.* **2001**, *148*, A730.
(22) West, K.; Zachauchristiansen, B.; Jacobsen, T.; Skaarup, S. *Electrochim. Acta* **1993**, *38*, 1215.
(23) Dong, W.; Rolison, D. R.; Dunn, B. *Electrochem. Solid-State Lett.* **2000**, *3*, 457.
(24) Chan, C. K.; Peng, H. L.; Twesten, R. D.; Jarausch, K.; Zhang, X. F.; Cui, Y. *Nano Lett.* **2007**, *7*, 490.
(25) Park, H. K.; Smyrl, W. H. *J. Electrochem. Soc.* **1994**, *141*, L25.

(26) Le, D. B.; Passerini, S.; Guo, J.; Ressler, J.; Owens, B. B.; Smyrl, W. H. *J. Electrochem. Soc.* **1996**, *143*, 2099.
(27) Pan, L. J.; Qiu, H.; Dou, C. M.; Li, Y.; Pu, L.; Xu, J. B.; Shi, Y. *Int. J. Mol. Sci.* **2010**, *11*, 2636.
(28) Novak, P.; Muller, K.; Santhanam, K. S. V.; Haas, O. *Chem. Rev.* **1997**, *97*, 207.
(29) Snook, G. A.; Kao, P.; Best, A. S. *J. Power Sources* **2011**, *196*, 1.
(30) Matsunaga, T.; Daifuku, H.; Kawagoe, T. *Nippon Kagaku Kaishi* **1990**, 1.
(31) Macdiarmid, A. G.; Epstein, A. J. *Synth. Met.* **1994**, *65*, 103.
(32) Krinichnyi, V. I. *Russ. Chem. Bull.* **2000**, *49*, 207.
(33) Ryu, K. S.; Kim, K. M.; Kang, S. G.; Lee, G. J.; Chang, S. H. *Solid State Ionics* **2000**, *135*, 229.
(34) Genies, E. M.; Hany, P.; Santier, C. *J. Appl. Electrochem.* **1988**, *18*, 751.
(35) Goto, F.; Abe, K.; Okabayashi, K.; Yoshida, T.; Morimoto, H. *J. Power Sources* **1987**, *20*, 243.
(36) Boschi, T.; Divona, M. L.; Tagliatesta, P.; Pistoia, G. *J. Power Sources* **1988**, *24*, 185.
(37) Macdiarmid, A. G.; Yang, L. S.; Huang, W. S.; Humphrey, B. D. *Synth. Met.* **1987**, *18*, 393.
(38) Li, C. Z.; Zhang, B. R.; Wang, B. C. *J. Power Sources* **1992**, *39*, 259.
(39) Bhadra, S.; Khastgir, D.; Singha, N. K.; Lee, J. H. *Prog. Polym. Sci.* **2009**, *34*, 783.
(40) Walk, C. R.; Margalit, N. *J. Power Sources* **1997**, *68*, 723.
(41) Livage, J. *Chem. Mater.* **1991**, *3*, 578.
(42) Dong, W.; Sakamoto, J.; Dunn, B. *J. Sol-Gel Sci. Technol.* **2003**, *26*, 641.
(43) Takahashi, K.; Wang, Y.; Cao, G. Z. *J. Phys. Chem. B* **2005**, *109*, 48.
(44) Wang, Y.; Takahashi, K.; Lee, K.; Cao, G. Z. *Adv. Funct. Mater.* **2006**, *16*, 1133.
(45) Passerini, S.; Chang, D.; Chu, X.; Le, D. B.; Smyrl, W. *Chem. Mater.* **1995**, *7*, 780.
(46) Baddour, R.; Pereiraramos, J. P.; Messina, R.; Perichon, J. *J. Electroanal. Chem.* **1991**, *314*, 81.
(47) Huguenin, F.; Giz, M. J.; Ticianelli, E. A.; Torresi, R. M. *J. Power Sources* **2001**, *103*, 113.
(48) Baddour, R.; Pereiraramos, J. P.; Messina, R.; Perichon, J. *J. Electroanal. Chem.* **1990**, *277*, 359.
(49) Mohan, V. M.; Hu, B.; Qiu, W. L.; Chen, W. *J. Appl. Electrochem.* **2009**, *39*, 2001.
(50) Leroux, F.; Goward, G.; Power, W. P.; Nazar, L. F. *J. Electrochem. Soc.* **1997**, *144*, 3886.
(51) Leroux, F.; Koene, B. E.; Nazar, L. F. *J. Electrochem. Soc.* **1996**, *143*, L181.
(52) Huguenin, F.; Torresi, R. M.; Buttry, D. A. *J. Electrochem. Soc.* **2002**, *149*, A546.
(53) Decher, G. *Science* **1997**, *277*, 1232.
(54) Decher, G.; Hong, J. D.; Schmitt, J. *Thin Solid Films* **1992**, *210*, 831.
(55) Lee, S. W.; Yabuuchi, N.; Gallant, B. M.; Chen, S.; Kim, B. S.; Hammond, P. T.; Shao-Horn, Y. *Nat. Nanotechnol.* **2010**, *5*, 531.
(56) Lee, S. W.; Gallant, B. M.; Byon, H. R.; Hammond, P. T.; Shao-Horn, Y. *Energy Environ. Sci.* **2011**, *4*, 1972.
(57) Hyder, M. N.; Lee, S. W.; Cebeci, F. Ç.; Schmidt, D. J.; Shao-Horn, Y.; Hammond, P. T. *ACS Nano* **2011**, *5*, 8552.
(58) Lutkenhaus, J. L.; Hammond, P. T. *Soft Matter* **2007**, *3*, 804.
(59) Michel, M.; Taylor, A.; Sekol, R.; Podsiadlo, P.; Ho, P.; Kotov, N.; Thompson, L. *Adv. Mater.* **2007**, *19*, 3859.
(60) Wang, D. G.; Wang, X. G. *Langmuir* **2011**, *27*, 2007.
(61) Zhang, X. Z. X.; Yang, W. S.; Evans, D. G. *J. Power Sources* **2008**, *184*, 695.
(62) Lee, S. W.; Kim, J.; Chen, S.; Hammond, P. T.; Shao-Horn, Y. *ACS Nano* **2010**, *4*, 3889.
(63) Huguenin, F.; Ferreira, M.; Zucolotto, V.; Nart, F. C.; Torresi, R. M.; Oliveira, O. N. *Chem. Mater.* **2004**, *16*, 2293.
(64) Ferreira, M.; Huguenin, F.; Zucolotto, V.; da Silva, J. E. P.; de Torresi, S. I. C.; Temperini, M. L. A.; Torresi, R. M.; Oliveira, O. N. *J. Phys. Chem. B* **2003**, *107*, 8351.
(65) Schweiss, R.; Zhang, N.; Knoll, W. *J. Sol-Gel Sci. Technol.* **2007**, *44*, 1.
(66) Chiang, J. C.; Macdiarmid, A. G. *Synth. Met.* **1986**, *13*, 193.
(67) Ryu, K. S.; Moon, B. W.; Joo, J.; Chang, S. H. *Polymer* **2001**, *42*, 9355.
(68) Cheung, J. H.; Stockton, W. B.; Rubner, M. F. *Macromolecules* **1997**, *30*, 2712.
(69) Pelletier, O.; Davidson, P.; Bourgaux, C.; Coulon, C.; Regnault, S.; Livage, J. *Langmuir* **2000**, *16*, 5295.
(70) Wood, K. C.; Zacharia, N. S.; Schmidt, D. J.; Wrightman, S. N.; Andaya, B. J.; Hammond, P. T. *Proc. Natl. Acad. Sci. U.S.A.* **2008**, *105*, 2280.
(71) Wang, Y.; Qian, W. P.; Tan, Y.; Ding, S. H.; Zhang, H. Q. *Talanta* **2007**, *72*, 1134.
(72) Li, G. C.; Pang, S. P.; Jiang, L.; Guo, Z. Y.; Zhang, Z. K. *J. Phys. Chem. B* **2006**, *110*, 9383.
(73) Wan, M. X.; Yang, J. P. *J. Appl. Polym. Sci.* **1995**, *55*, 399.
(74) Ferreira, M.; Zucolotto, V.; Huguenin, F.; Torresi, R. M.; Oliveira, O. N. *J. Nanosci. Nanotechnol.* **2002**, *2*, 29.
(75) Porcel, C.; Lavalle, P.; Ball, V.; Decher, G.; Senger, B.; Voegel, J. C.; Schaaf, P. *Langmuir* **2006**, *22*, 4376.
(76) Lavalle, P.; Gergely, C.; Cuisinier, F. J. G.; Decher, G.; Schaaf, P.; Voegel, J. C.; Picart, C. *Macromolecules* **2002**, *35*, 4458.
(77) Picart, C.; Mutterer, J.; Richert, L.; Luo, Y.; Prestwich, G. D.; Schaaf, P.; Voegel, J. C.; Lavalle, P. *Proc. Natl. Acad. Sci. U.S.A.* **2002**, *99*, 12531.
(78) Hu, Y. S.; Liu, X.; Muller, J. O.; Schlogl, R.; Maier, J.; Su, D. S. *Angew. Chem., Int. Ed.* **2009**, *48*, 210.
(79) Srinivasan, S.; Pramanik, P. *Synth. Met.* **1994**, *63*, 199.
(80) Akl, A. A. *J. Phys. Chem. Solids* **2010**, *71*, 223.
(81) McAloney, R. A.; Sinyor, M.; Dudnik, V.; Goh, M. C. *Langmuir* **2001**, *17*, 6655.
(82) Schoeler, B.; Poptoschev, E.; Caruso, F. *Macromolecules* **2003**, *36*, 5258.
(83) DeLongchamp, D. M.; Kastantin, M.; Hammond, P. T. *Chem. Mater.* **2003**, *15*, 1575.
(84) Richert, L.; Lavalle, P.; Payan, E.; Shu, X. Z.; Prestwich, G. D.; Stoltz, J. F.; Schaaf, P.; Voegel, J. C.; Picart, C. *Langmuir* **2004**, *20*, 448.
(85) Sun, B.; Jewell, C. M.; Fredin, N. J.; Lynn, D. M. *Langmuir* **2007**, *23*, 8452.
(86) Patil, A.; Patil, V.; Shin, D. W.; Choi, J. W.; Paik, D. S.; Yoon, S. J. *Mater. Res. Bull.* **2008**, *43*, 1913.